MARS/MOON CRATERING RATE RATIO ESTIMATES

BORIS A. IVANOV
Institute for Dynamics of Geospheres, Russian Academy of Sciences, Moscow, Russia 117939

Received: 1 November 2000; accepted: 26 February 2001

Abstract. This article presents a method to adapt the lunar production function, i.e. the frequency of impacts with a given size of a formed crater as discussed by Neukum *et al.* (2001), to Mars. This requires to study the nature of crater-forming projectiles, the impact rate difference, and the scaling laws for the impact crater formation. These old-standing questions are reviewed, and examples for the re-calculation of the production function from the moon to Mars are given.

1. Crater Forming Projectiles

The modern crater forming projectiles are believed to be presented by three main populations: asteroids, Jupiter-Family comets (JFC), and long period comets (LPC). These bodies have different kinds of orbits, and physical and mechanical properties. According to Shoemaker and Wolfe (1982), for Earth and for all terrestrial planets the JFC impacts play a minor role in the formation of impact craters. Asteroids and long period comets may give comparable contributions to the modern cratering rate. However, the long period comets' flux in terms of mass of the projectiles is currently poorly known. Shoemaker and Wolfe (1982) used measurements of the LPC nuclear size by Roemer (1965, 1966), Roemer and Lloyd (1966) and Roemer *et al.* (1966), and the astronomically estimated frequency of fly-by through the solar system. As the estimated cratering rate from these assumptions was too high, Shoemaker and Wolfe (1982) ascribed the overestimate to the unresolved comae of measured LPCs, and drastically decreased the published nuclear diameter estimates by a factor of 3. Consequently, knowing the average probability and velocity of LPC impacts very well, there remains a severe problem of not knowing both the size distribution and the formation rate of impact craters by LPCs.

According to Neukum *et al.* (2001), the size-frequency distribution (SFD) of craters at best corresponds to the one of asteroids. At the same time, known estimates for the SFD of comet nuclei contradict the planetary cratering records (Shoemaker and Wolfe, 1982). Thus, as a first approximation this article compares the moon and Mars only for asteroid impacts.

Most asteroids occupy the area between the orbits of Mars and Jupiter, named the Main Belt (MB; see Binzel *et al.*, 1989, for a review and database). The relatively small sub-population of asteroids that currently cross the orbits of terrestrial planets are called *Planet Crossing Asteroids (PCA)*.

Chronology and Evolution of Mars **96** 87–104, 2001.

Recently, Morbidelli (1999) has reviewed the evolution of understanding the PCA origin. The first scenario developed by Wetherill (1979, 1988) and interpreted by Greenberg and Nolan (1989, 1993) assumes the catastrophic collision's fragment injection to resonance phase space area. Being in a resonance (ν_6 or 3/1), "new" fragmental asteroids change eccentricities and become PCAs. They further change orbits due to close encounters with terrestrial planets. The time scale for the transition from MB to PCA orbits is $\sim$1 Myr; the life time at the PCA's orbits is tens of Myr. If Mars alone controls the orbit evolution, an asteroid begins to cross the Earth orbit in 100 Myr ("slow track"). If Earth removes an asteroid from a resonance, the orbit evolves 10 to 100 times faster (1 to 10 Myr, "fast track").

Later, the "solar sink" was found to be an important mechanism to limit the time scale of the orbital evolution due to resonances. A chain of papers after Farinella *et al.* (1994), reviewed by Morbidelli (1999), demonstrated that resonances "pump" eccentricities of PCAs up to a sun-grazing orbit. The recent dynamic model by Gladman *et al.* (1997) predicts a median lifetime of 2 Myr for MB asteroids in resonant orbits, while 90% will impact Sun or planets, or will be ejected out of the inner solar system within 10 Myr. The short lifetime implies a very intensive re-supply of PCAs from the rest of the MB asteroids. The pure resonant orbital evolution thus looks like an effective "fast track" to create PCAs from MB asteroids.

The "slow track" interpretation was renovated by Migliorini *et al.* (1998) and Morbidelli (1999): Multiple weak resonances lead to chaotic evolution of the MB asteroids' orbits that are far from main mean motion and secular resonances with Jupiter and Saturn. These orbits "migrate" in phase space with a good chance to become Mars-crossing orbits on a timescale of 25 Myr. Then, Mars-crossers will evolve to PCAs by close encounters with Mars and other terrestrial planets.

Regarding planetary cratering rate estimates, three comments are important:

1. Before numerical models have accumulated better statistics in the behavior of small bodies in the solar system, the natural axiom assumed that the currently observed PCAs present a sensible "time slice" of a stationary distribution of orbital elements, so that impact probabilities and impact velocities of asteroids can be estimated from currently observed PCAs. With help of scaling laws the cratering rate is estimated. Most of the currently observed asteroids never hit any planet. The time to impact for a typical orbit is about $0.1 - 1$ Gyr. Thus, 4 to 10 "generations" of asteroids should replace one another on the same PCA orbits to create a new crater on one of the terrestrial planets or their satellites.
2. The "fast track" with ejection due to catastrophic collision differs from the "slow track", which operates equally for bodies of any size. The fragmentation ejection into resonant orbits may change the SFD of fragments. Smaller fragments are ejected faster, so that the "fast track" population of PCAs should be more abundant in small bodies compared to the MB population. In terms of a close to power law SFD, the PCA's SFD is "steeper" than the MB SFD.
3. Non-gravitational forces (such as the Yarkovsky effect) also can result in a steeper SFD for PCAs.

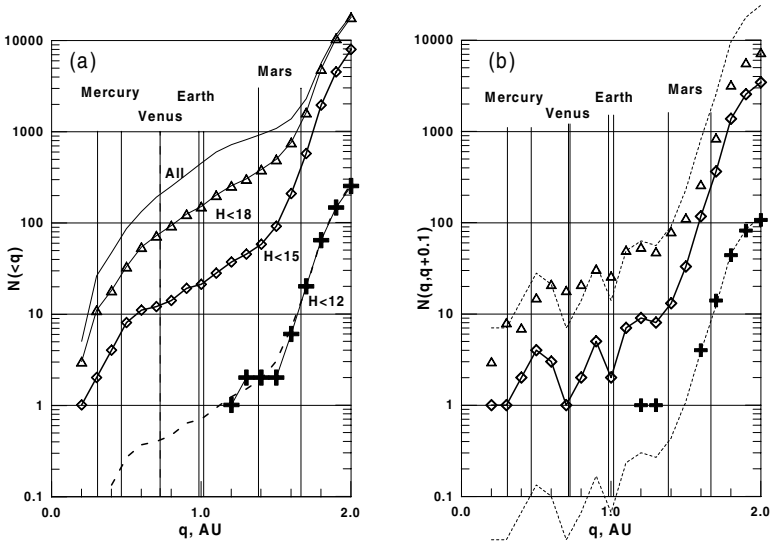

Figure 1. Cumulative (a) and incremental (b) perihelion distribution of planetary crossing asteroids (PCAs) of different size (characterized by magnitude H). The $N(q)$ dependence of PCAs with $H < 15$ compromises the completeness of observation and the numerosity at near-Earth orbits.

Below we assume that asteroids from the MB may be treated as best candidates for the cratering rate comparison. Cometary input is not included in our current estimates. We also assume that the currently observed population of PCA is stationary (at least for the last 3 Gyr). For more ancient periods, e.g. the end of the heavy bombardment period, we assume that the relative cratering rates on terrestrial planets in respect to the moon was the same as relative cratering rates for the currently observed PCA. Each of these assumptions should be taken with care.

2. Projectile Flux Estimate

In the approach of Shoemaker and Wolfe (1982) for short period comets, the set of observed comet orbits is sorted in perihelion distance q, from which the average impact probability and velocity are estimated. This way, observed orbits are assumed to represent an ensemble of a statistically "averaged" steady-state population of PCAs. Here, the list of osculating orbits "astorb.dat", presented on *http://asteroid.lowell.edu* (February 2000), is used.

To remove bias in the observed asteroid population, several techniques have been developed (e.g., Rabinowitz, 1993, 1997; Rabinowitz *et al.*, 1994; Jedicke and Metcalfe, 1998; Bottke *et al.*, 2000a, b). Here, PCAs are sorted in their absolute magnitude and the obvious bias in the q-distribution is removed. Figure 1 plots "incremental" and "cumulative" distributions of the number of PCAs of different size, presented by magnitude. The incremental number of asteroids is calculated

as their number per q-bin of width 0.1 AU. Comparing q-distributions of asteroids with $H < 15$ and $H < 12$ reveals similar behavior close to the Mars orbit.

The observations for Mars-crossers with $H < 15$ appear to be relatively complete, agreeing with theory (Bottke *et al.*, 2000b). A scaled curve derived from $N(q)$ distributions for $H < 15$ (Figure 1) and larger bodies fits to the data of $N(q)$ for larger bodies with $H < 12$. For Mars-crossers $N(q)$ functions look similar. For small q the number of $H < 12$ asteroids drops below 1. This means that the steady-state number of large NEAs is less than 1 – the delivery rate is smaller than the lifetime of large bodies, and they only sporadically appear in the Earth's vicinity. Here, it is assumed that the q-distribution of asteroids with $H < 15$ may be used to estimate the $N(q)$ function for smaller bodies.

The completeness of observation of small bodies on near Earth orbits (NEA) is now estimated as 40% for $H < 18$ (Bottke *et al.*, 2000b). At the same time, the trial fit of $N_{18}(q)$ with the $N_{15}(q)$ curve shows a more or less similar behavior for PCAs. A first order correction for PCAs is obtained by multiplication by some factor close to 2.5, according to Bottke *et al.* (2000b). For Mars-crossers with $H < 18$ the observational bias obviously increases for larger q (Figure 1).

With the procedure described above the impact rates on the moon and Mars are compared. Impact velocities and probabilities for all Earth crossers with $H < 18$, and for all Mars-crossers with $H < 15$ are calculated. To compare absolute impact rates on Mars and the moon, Mars estimates for each q are multiplied with the ratio $N_{H<15}/N_{H<18}$. This implies that unobserved Earth and Mars-crossers should have orbits similar to currently observed bodies. Figure 2 illustrates the impact velocity distribution for Mars and the moon binned in intervals of 1 km/s.

The Öpik formulas, refined by Wetherill (1967) for the general case of elliptic orbits for both target and projectile, are applied to all bodies in the "astorb.dat" file. A random orientation of the nodes latitude is assumed, so that all mutual positions of inclined elliptical orbits have the same probability. For each target (Mars or the moon) and projectile (PCA) the impact probability and velocity are calculated. The *total* impact probability, corrected for observational bias for small Mars-crossers, and the *average* impact velocity are needed to compute the cratering rate.

Before determining size-frequency distributions of projectiles, it helps to compare the estimated impact rate of asteroids of equal size on the moon and Mars.

For the moon the *average* probability of impact of *observed* NEA with $H < 18$ is 1.9×10^{-10} yr^{-1}. For the total number of projectiles of 155 and the moon radius of 1732 km the average impact rate (AIR) per year per km^2 is $AIR_{\rm moon} = 0.77 \times 10^{-15}$ yr^{-1} km^{-2} The average impact velocity is $\langle v_{\rm moon} \rangle = 16.2$ km/s.

The AIR estimate is difficult for Mars, because its orbit's eccentricity varies in the range of $\sim 0.01 - 0.1$ with a period of 2 Myr (Ward, 1992). Currently, this eccentricity is close to the upper limit $e = 0.094$, and Mars' distance to the Sun varies in the range $\sim 1.4 - 1.7$ AU. Figure 1 shows, how the number of Mars crossers grows with q within limits of the current Mars aphelia and perihelia: The number of potential impactors is 20 times larger in the aphelia than in the perihelia.

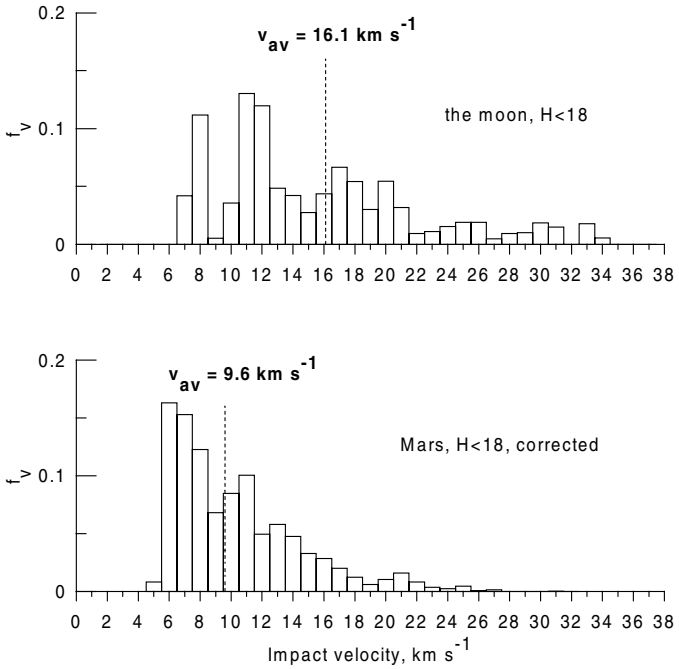

Figure 2. The impact velocity distribution for the moon and Mars (fraction of impacts per 1 km/s).

The calculations with "astorb.dat" Mars crossers show that the impact rate changes 7 times each Martian year, defining **"impact seasons"**.

For this reason, the AIR for Mars may either be calculated for shorter periods assuming a specific eccentricity, or may be averaged for one Martian year or even for the cycle of the Martian orbit eccentricity variation of $\sim$2 Myr. The long-time average, corrected for the unobserved $H < 18$ Mars crossers, is estimated as

$$AIR_{\rm Mars} = 1.57 \times 10^{-15} {\rm yr}^{-1} {\rm km}^{-2} \, .$$

The average impact velocity is $\langle v_{\rm Mars} \rangle = 8.62 \, {\rm km \, s}^{-1}$.This number corresponds to the observed NEA with $H < 18$, and may present $\sim$40% of the real impact rate, as discussed above.

The Mars/moon impact rate ratio, averaged in time, called "$R_{\rm bolide}$" or $R_{\rm b}$ following Hartmann and Neukum (2001), has a value

$$R_{\rm b} = AIR_{\rm Mars}/AIR_{\rm moon} = 1.57/0.77 = 2.04 \qquad (1)$$

for asteroids *of the same size*. This is the ratio of frequencies of impacts per unit area. Due to the larger total surface of Mars, the ratio of the absolute numbers of impacts is larger than the value of Equation (1).

To convert this ratio, $R_{\rm bolide}$, to the average cratering rate ratio, R, one needs to know the scaling law for impact cratering due to the different impact velocities

and surface gravity on the moon and Mars, and the size-frequency distribution of projectiles to estimate the R value for *equal crater diameters*.

3. Scaling Laws

Crater diameters for the impact of the same projectile on the moon and on Mars depend on the efficiency of the cratering at different impact velocity and surface gravity. Nowadays, the scaling law by Schmidt and Housen (1987) is widely used, which conveniently is written as

$$D_t = 1.16(\delta/\rho)^{1/3} D_P^{0.78} (v \sin\alpha)^{0.43} g^{-0.22} \quad (2)$$

where D_t is the transient crater diameter, D_P is the projectile diameter, ρ and δ are densities of target and projectile materials, v is the impact velocity, α is the impact angle, and g is the gravity acceleration (e.g., Pierazzo *et al.*, 1997). For simple craters formed in the gravity regime their final diameter is about D_t.

The power law (Equation 2) may be more complex in extreme cases of small strength craters ($D < 50$ to 300 m (see Neukum and Ivanov, 1994), and large modified (collapsed) craters (see the review by Melosh and Ivanov, 1999).

The strength-to-gravity transition may be incorporated into the scaling law following Schmidt and Housen (1987), Neukum and Ivanov (1994), and Ivanov*et al.* (2000). Equation (2) may be rewritten in a form, where for sufficiently small events the crater diameter is directly proportional to the projectile diameter:

$$\frac{D_t}{D_P[(\delta/\rho)^{1/3}(v \sin\alpha)^{0.43}]^{0.78}} = \frac{(1.16)^{1/0.78}}{[(D_{sg} + D_t)g]^{0.22/0.78}} \quad ,$$

where D_{sg} is the characteristic strength to gravity transition crater diameter; craters with $D_t \ll D_{sg}$ are formed in a strength regime, while craters with $D_t \gg D_{sg}$ are formed in a gravity regime. After this reduction the generalized form of the scaling law is

$$\frac{D_t}{D_P(\delta/\rho)^{0.26}(v \sin\alpha)^{0.55}} = \frac{1.28}{[(D_{sg} + D_t)g]^{0.28}} \quad . \quad (3)$$

The scaling law (Equation 3) gives a smooth transition from the gravity cratering regime (Equation 2) to the assumed strength cratering regime where (for $D_t \ll D_{sg}$) the crater diameter is proportional to the projectile size:

$$D_t = \frac{1.28}{(D_{sg}g)^{0.28}} D_P(\delta/\rho)^{0.26}(v \sin\alpha)^{0.55} \quad .$$

Such a model assumes that the formation of a small crater on a planetary surface may be described as the cratering process in a target with a constant strength. In reality, the strength of near surface rocks may be highly variable due to the presence

of a regolith and a megaregolith. However, Equation (2) gives an upper limit for the crater size for a given projectile, implicitly assuming a low cohesion nature of shuttered and weathered near-surface rocks. Equation (3) gives a lower limit of the crater size, provided the near surface rocks have some finite cohesion.

The gravity collapse of a transient cavity makes the diameter of a final modified crater larger in comparison with a hypothetical simple crater which would be created by the same impact in the absence of the gravity collapse. For simple estimates one can use the semiempirical model derived by S. Croft (1985; see also Chapman and McKinnon, 1986) to find the transient cavity diameter, D_t, for an observed crater with a rim diameter D:

$$D_t = D_*^{0.15} \times D^{0.85} \tag{4}$$

for $D > D_*$. The value of a critical diameter D_*, which defines the boundary crater diameter when the collapse begins, depends on the target material strength and gravity. On Earth, the value of D_* is ~4 km for crystalline rocks. For other terrestrial planets D_* varies approximately inversely proportional to the surface gravity acceleration (Pike, 1980). Using Equation (4) to estimate D_t, and Equation (3) for an assumed impact velocity v and impact angle α, one can estimate a projectile diameter needed to form the crater with a given final diameter D.

The best test for the model is to compare the theoretical and observed volume of the impact melt in well studied terrestrial impact craters. Numerical models of the impact events enable to estimate the impact melt volume. The results are confirmed by real underground nuclear tests. The reasonably good coincidence (Figure 3) between theory and observations gives confidence in the validity of scaling laws presented here (Ivanov, 1981; Pierazzo *et al.*, 1997).

The general review of the simple-to-complex transition has been published by Pike (1980). Most of these data reflect boundary diameters between ranges of different morphology styles of impact craters. In general, it is hard to say what is the best value of D_* in Equation (4) to estimate the crater diameter increase due to modification on a given planetary body. As a first approximation for terrestrial planets one may use the inverse proportionality of D_{sg} and D_* to gravity g (Pike, 1980). The recent Mars Global Surveyor data seem to significantly improve the D_* estimates (Garvin *et al.*, 2000).

4. Cratering Rate Comparison

The rigorous procedure of the interplanetary comparison of crater records consists of several natural steps.

1. Calculate the shape of the size-frequency distribution of projectiles using one of the bodies as a reference.
2. Calculate the production curve for new impact velocities and surface gravity, assuming the SFD of projectiles for the other planet is the same as for the reference planetary body.

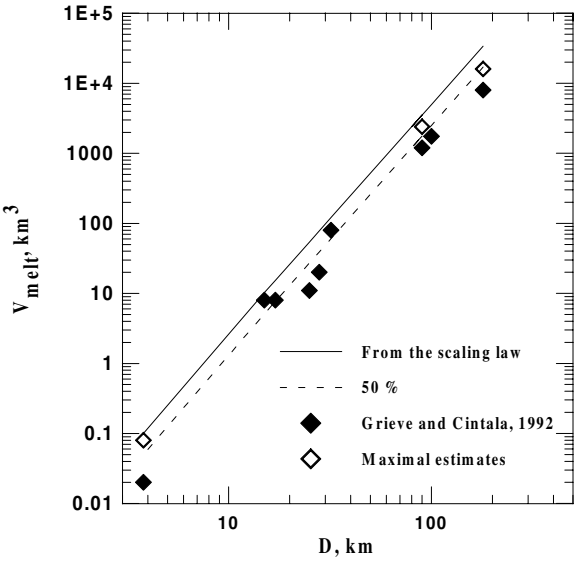

Figure 3. Comparison of calculated (Ivanov, 1981; Pierazzo *et al.*, 1997) and observed (Grieve and Cintala, 1992) impact melt volumes in terrestrial craters. The solid line shows the total theoretical melt production, the dashed line corresponds to an assumption that 50% of the produced impact melt is ejected beyond the crater rim.

3. Normalize the production function to the average impact rate ratio.

The known lunar production function is discussed by Neukum*et al.* (2001). The re-calculations of the Hartmann Production Function (HPF) and the one of Neukum (NPF) for the case of Mars are presented below. However, before discussing the relatively accurate procedure, some order-of-magnitude estimates are made.

Model 0 uses power law functions for both the cratering scaling law and the projectile SFD, and assumes one (average) impact angle and one (average) impact velocity. This was the first successful technique to compare impact cratering rates throughout the solar system (Hartmann, 1977; Hartmann*et al.*, 1981). In this model, the SFD as function of the projectile's diameter D_{P} is written as:

$$N(>D_{\mathrm{P}}) \sim D_{\mathrm{P}}^{-n} \tag{5}$$

The crater diameter is expressed as

$$D \sim D_{\mathrm{P}}^{\alpha} v^{\beta} g^{-\gamma}.$$

The crater's SFD is also a power law

$$N(>D) \sim D^{-b} \tag{6}$$

where $b = n/\alpha$. For a known ratio of numbers of impacts of projectiles of a given size at a given area during a given time (named R_{b} in Equation 1), one can derive the ratio of cratering rates for a given crater diameter. Due to differences in the

impact velocity and surface gravity, craters of the *same diameter* are formed by projectiles of *different size*. On planet #1 (let it be Mars) the crater of a diameter D is created by a projectile with a diameter

$$D_{\mathrm{PM}} = D^{1/\alpha} v_{\mathrm{M}}^{-\beta/\alpha} g_{\mathrm{M}}^{\gamma/\alpha}$$

On planet #2 (the moon) the same crater is created by a projectile with the diameter

$$D_{\mathrm{Pm}} = D^{1/\alpha} v_{\mathrm{m}}^{-\beta/\alpha} g_{\mathrm{m}}^{\gamma/\alpha}$$

Mars gravity is larger, and the average impact velocity is smaller than on the moon. Consequently, a larger projectile needs to strike Mars to create the same crater. Larger bodies are less numerous (Equation 5), and the ratio of the cratering rate, R, is smaller than the ratio of impact rates, R_{b}, by a "planetary" factor, f_{P}, derived from the scaling law and the size-frequency distributions:

$$f_{\mathrm{P}} = (v_{\mathrm{M}}/v_{\mathrm{m}})^{b\beta/\alpha} \cdot (g_{\mathrm{M}}/g_{\mathrm{m}})^{-b\gamma/\alpha}$$

The final ratio of cratering rates (Mars/moon ratio, R) is given by the expression

$$R = f_{\mathrm{P}} R_{\mathrm{b}}$$

To make a bridge to previous estimates for interplanetary comparison of crater population, we test first "old" exponents, used by Hartmann (1977) and Hartmann *et al.* (1981): $\beta = 2/3.3 = 0.606$, $\gamma = 0.2$. For these parameters the ratio of crater diameters on Mars and the moon for velocities estimated above is

$$D_{\mathrm{M}}/D_{\mathrm{m}} = (v_{\mathrm{M}}/v_{\mathrm{m}})^{\beta} (g_{\mathrm{M}}/g_{\mathrm{m}})^{-\gamma} = 0.694 \tag{7}$$

The "planetary" factor, f_{P}, depends on the SFD's steepness (Equations 5 or 6).

For typical values of $b = 2$ to 3 the Mars/moon cratering rate ratio R varies in the range

$$R = (D_{\mathrm{M}}/D_{\mathrm{m}})^{b} \times R_{\mathrm{b}} = (0.33 \text{ to } 0.48) \times 4.8 = 1.6 \text{ to } 2.3 \tag{8}$$

"Modern" values of exponents in the scaling law ($\beta = 0.43$, $\gamma = -0.22$ (Equation 2) give close numbers for simple gravity craters:

$$D_{\mathrm{M}}/D_{\mathrm{m}} = (v_{\mathrm{M}}/v_{\mathrm{m}})^{\beta} (g_{\mathrm{M}}/g_{\mathrm{m}})^{-\gamma} = 0.64 \tag{9}$$

$$R = (D_{\mathrm{M}}/D_{\mathrm{m}})^{b} \times R_{\mathrm{b}} = (0.26 \text{ to } 0.41) \times 4.8 = 1.28 \text{ to } 1.99 \tag{10}$$

This comparison leads to the conclusion that the "old" scaling by Hartmann (1977) gives just the same $D_{\mathrm{M}}/D_{\mathrm{m}}$ as more recent scaling laws for *simple* craters. The variations in scaling exponents and average impact velocities derived here are close to compensate one another. The "typical" impact on Mars creates the crater 1.5 times smaller than on the moon. Consequently, the cratering rate ratio is less than the average impact rate ratio.

TABLE I

Cratering rate comparison for simple craters for different values of the Mars orbit eccentricity, e, and time averaged estimates for the period of 2 Myr. M=Mars; m=moon; R_b is the Mars/moon impact rate ratio; $D_{D_P=1}$ is the crater diameter for vertical impact of an asteroid of 1 km diameter; b is the exponent in the cumulative size distribution (Equation 6).

Planet	v kms^{-1}	R_b	$D_{D_P=1}$ km	$b = 1.8$ $\left(\frac{D_M}{D_m}\right)^b$	R	$b = 2.2$ $\left(\frac{D_M}{D_m}\right)^b$	R	$b = 3.82$ $\left(\frac{D_M}{D_m}\right)^b$	R
moon	16.09		15.32						
Mars									
$e = 0.093$	8.61	4.8	9.87	0.45	2.18	0.38	1.83	0.19	0.90
$e = 0.05$	10.32	2.02	10.65	0.52	1.05	0.45	0.91	0.25	0.51
$e = 0.01$	10.86	1.73	10.88	0.54	0.93	0.47	0.81	0.27	0.47
Time av.	**9.59**	**2.04**	**10.32**	**0.49**	**1.00**	**0.42**	**0.86**	**0.22**	**0.45**

Taking into account the variation of the Mars orbit eccentricity, one can derive R-values for different slopes of the cumulative SFD providing the *same* steepness of the cratering curve. The data in Table I well represent possible ranges of R-values for different Mars orbits and the crater cumulative distribution steepness. For the current Mars orbit (high e) the R value is in the range $0.9-2.2$ for different ranges of the $N(>D)$ distribution. During time periods, when the Mars orbit is almost circular, R decreases to values in the range $0.5-0.9$.

The last section of Table I shows the time averaged cratering rate ratio R for sinusoidal variation of e with time and for varying $N(>D)$ steepness: R is in the range $0.45-1.0$, providing one compares SFD brunches with the *same steepness* m. One cannot compare the number of craters on Mars and the moon for diameter ranges where $N(>D)$ curves have different steepness.

The possible celestial source of uncertainty in these estimates is connected with possible modulation of the Mars crossers orbital evolution with the evolution of the eccentricity of the Martian orbit. This modulation in principle may shift the orbital distribution of Mars crossers, which may shift time averaged impact velocity and probability for Mars. However, the time scale of the Mars orbit variation is about 2 Myr (Ward, 1992), while the typical time scale for Mars crossers evolution is about 30 Myr (Migliorini *et al.*, 1998; Morbidelli, 1999).

Model 0 gives a proper general estimate for the values of the Mars/moon cratering rate ratio R due to the bombardment of asteroids. If comets have not the significant input into the cratering rate (see Neukum *et al.*, 2001), it can be concluded that the cratering rates on Mars and the moon are close within a factor of

1.5. For steep $N(D)$ distributions $R \approx 0.5$, in a shallow $N(D)$ diapason, R may be close to 1.0, if averaged over the time variation of the Martian eccentricity.

The general information given above enables to construct the predictive $N(D)$ functions for Martian surfaces of varying ages, as presented in the following.

Model 1 is a simple approach (e.g., Neukum and Ivanov, 1994) to assume that all impact craters are created with projectiles having one (average) impact velocity and one (average) impact angle of 45°.

In this case, the production functions, HPF and NPF, can be easily recalculated from the moon to Mars. The procedure includes the estimate of the projectile SFD using Equations (2 – 3). The derived projectile population is assumed to strike Mars with the proper larger intensity. Using the average impact velocity for Mars, the correspondent crater population and the Martian production curve are estimated. It is important to take into account that the simple-to-complex transition on Mars occurs at smaller critical diameter $D_* = 7$ km (Garvin *et al.*, 2000), while on the moon we assume the D_* value of 15 km (Pike, 1980).

Model 2 is more complex but more exact. It automatically takes the change of crater scaling into account, which happens in different diapasons of crater diameters at planetary bodies with different gravity and surface mechanical properties. The most straightforward way is to derive the model SFD for one body and then include the variation of impact and target parameters to compute the crater SFD on the other body. The technical problem arises from the fact that craters of the same diameter may be created by impacts of projectiles of varying size depending on their impact angle and velocity.

With an analytical expression for the SFD the problem is solved in a more rigorous style. Ivanov (1999) and Ivanov *et al.* (1999, 2000) have estimated the relationship between projectile and crater SFDs using the real observed velocity distribution of asteroids. The model assumes that:

- The crater diameter is some function, i.e. the scaling law, $D = D(D_P, v, \alpha)$ of the projectile and impact parameters D_P (projectile diameter), v (impact velocity) and α (impact angle, $\alpha = 90°$ means vertical impact).

- The probability for a projectile to have the impact velocity in the range from v to $v + dv$ is $f_v(v)dv$. The minimum impact velocity is equal to the escape velocity of a planetary body, v_{esc}. The maximum velocity depends on the orbital parameters of a target body and projectiles.

- The share of impacts in the range of angles from α to $\alpha + d\alpha$ is a function $f_\alpha(\alpha)$. The maximum impact angle is naturally 90° (vertical impact). The minimum angle of impact α_{min} is defined as an angle, below which craters become elongated. From the restricted amount of experimental data (Gault and Wedekind, 1978) $\alpha_{min} = 15°$ can be estimated. Bottke *et al.* (2000c) recently have confirmed an angle of order 12° as the upper boundary for a significant ellipticity of impact craters.

Any crater of a diameter D may be formed by impact of projectiles of various diameters, depending on the impact velocity and impact angle. In differential form this condition is expressed as

$$\frac{dN}{dD} = \int_{v_{\min}}^{v_{\max}} dv \int_{\alpha_{\min}}^{\alpha_{\max}} d\alpha \left[\frac{dN}{dD_{\mathrm{P}}} \frac{dD_{\mathrm{P}}}{dD} \right] f_v(v) f_\alpha(\alpha) \quad , \tag{11}$$

where both values in square brackets should be calculated for the projectile diameter $D_{\mathrm{P}}(D, v, \alpha)$, i.e. for the projectile of diameter D_{P}, which creates the crater of diameter D, impacting with velocity v at angle α.

The integral equation (11) enables to calculate the projectile SFD for a known SFD of craters, $D_{\mathrm{P}}(D, v, \alpha)$, and velocity and angular distributions of impact events. Then, Equation (11) gives the model impact crater SFD (a production function) for a given planetary surface from the projectile SFD and the impact velocity spectra.

Scaling laws (Equations 2, 4) simplify the procedure. The analytical fit to the lunar data derived by Neukum (1983) and recently improved by Ivanov (1999) and Ivanov *et al.* (2000) is one example; however, the general equation (11) may be applied for any input crater distribution. The resulting projectile SFD is also presented as a polynomial function similar to Neukum's lunar production function. From the derived projectile (asteroid) SFD the model SFD for Martian craters is calculated. Note however, that the same asteroid SFD for Earth-crossers and Mars-crossers is assumed. This may not be completely true, if non-gravity effects change, depending on asteroid size, the populations of fast and slow track delivery routes.

Results. With all the assumptions and simplifications described above, the model results in a Mars-to-moon re-calculation of the production functions.

The *Hartman Production Function (HPF)*, recalculated to Mars using **Model 2**, is shown in Figure 4 in comparison with the original lunar HPF. Figure 5 plots the Mars-to-moon ratio for the same crater diameter bins. In the spirit of the lunar HPF, the production function for Mars may be split into 3 power law branches (for an "average" lunar mare surface of ~3.4 Gyr on Neukum's time scale):

$$\begin{aligned} \log N_{\mathrm{H}} &= -2.894 - 3.82 \log D_{\mathrm{L}}, \quad D < 1.0 \text{ km} \\ \log N_{\mathrm{H}} &= -2.938 - 1.72 \log D_{\mathrm{L}}, \quad 1.0 \text{ km} < D < 32 \text{ km} \\ \log N_{\mathrm{H}} &= -2.146 - 2.20 \log D_{\mathrm{L}}, \quad D > 32 \text{ km} \end{aligned} \tag{12}$$

Note the slight change in the exponent (Equation 12) with respect to the lunar HPF (Neukum *et al.*, 2001). As Martian craters created with the same projectile are smaller than on the moon, the boundary diameters of different power law branches are shifted to smaller sizes compared to the lunar HPF (Equation 1).

As the HPF is presented as the 3 power relationships (Neukum *et al.*, 2001), the Mars-to-moon ratio has specific values for each power branch (Figure 5). The smaller crater dimensions on Mars for the same projectile diameter and the higher Martian impact rate barely compensate each other for $D > 2$ km. Thus, the Mars-to-moon crater number ratio is close to unity with the accuracy of ±20%.

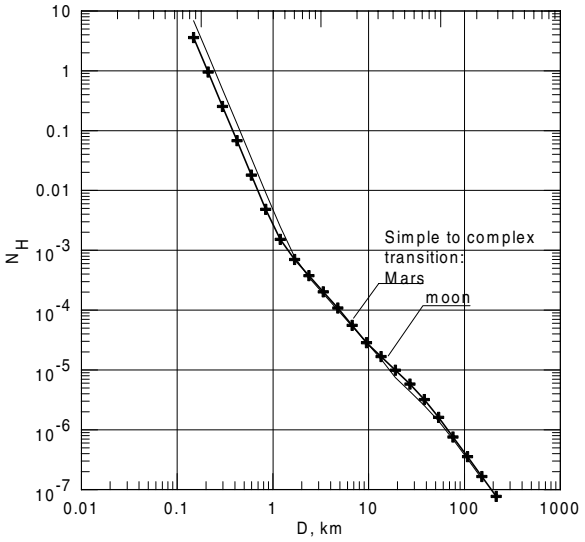

Figure 4. The Hartman production function for Mars in comparison with the lunar prototype. Crosses are plotted against the middle of $2^{1/2}$ diameter bins.

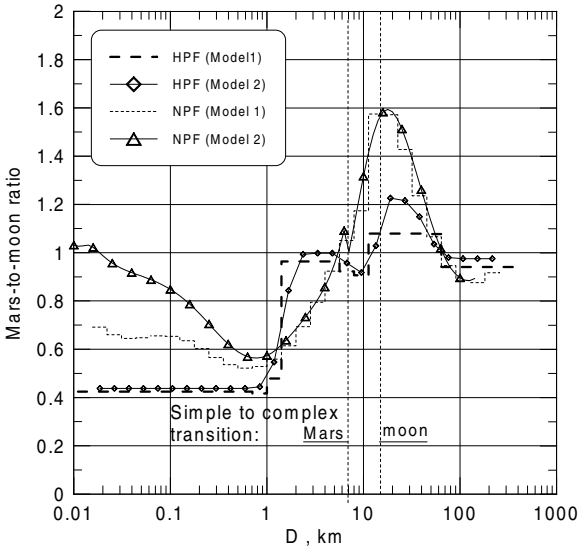

Figure 5. The Mars-to-moon ratio of a number of impact craters with equal diameter. Hartmann Production Function (HPF) and Neukum Production Function (NPF) are recalculated from the moon to Mars using **Model 1** (one average impact velocity and one average impact angle of 45°) and **Model 2** (the full ensemble of impact velocities and impact angles). All re-calculations except NPF (**Model 2**) use the gravity crater scaling law with the Croft's collapse model. The NPF (**Model 2**) is recalculated assuming the strength-to-gravity cratering regime transition with D_{sg} at 300 m on the moon and 100 m on Mars. For details see text.

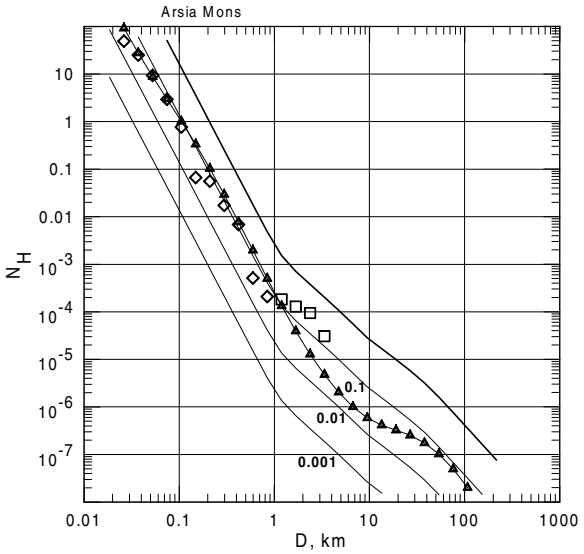

Figure 6. Martian "isochrones" based on the Hartmann Production Function (HPF) compared to the crater counts on the Arsia Mons volcano (*square*) and at its summit caldera floor (*diamonds*) by Hartmann (1999). The upper curve corresponds to the same age as the "average lunar mare" (∼3.4 Gyr). Also shown are "isochrones" for surfaces that accumulated 1/10, 1/100, and 1/1000 less craters. The Arsia Mons caldera floor accumulated roughly 10 times less craters than surfaces of lunar mare "average" age. The NPF, derived below, is shown for comparison (*small triangles*).

The lunar HPF is constructed for the "average mare" surface age, estimated above as ∼3.4 Gyr. If no excessive accuracy is required, the Martian HPF for various crater retention ages may be given as fractions of the "average mare" crater density. Figure 6 illustrates these HPF "isochrones" for Martian surfaces with 1/10 and 1/100 of the "average mare" crater counts. The recent MGS data for the caldera of Arsia Mons (Hartmann, 1999) corresponds to a crater areal density of 1/10 of the "average lunar mare". Martian crater counts are discussed by Hartmann and Neukum (2001), and Table II presents numerical values of the HPF for Mars.

The *Neukum Production Function (NPF)* originally is presented in the cumulative form, from which the incremental and R-plot distributions are easily produced. Figure 7 compares the Martian NPF for a 1 Gyr-old surface with the lunar NPF of the same age. Figure 5 shows this comparison in more detail, as the ratio of incremental number of craters in the same diameter intervals. The non-power law NPF has a steepness that differs from the HPF power law. Consequently, the Mars-to-moon ratio varies in a wider range.

The NPF may be approximated as a polynomial similar to the lunar NPF:

$$\log_{10}(N) = a_0 + \sum_{n=1}^{11} a_n \left[\log_{10}(D)\right]^n \ .$$

Coefficients a_i are listed in Table III; the fit is valid for $\sim 15 \text{ m} < D < 362$ km.

TABLE II

Calculated crater number in each crater diameter bin for Mars and the moon according to Hartmann's (HPF) and Neukum's Production Function (NPF) for an age of the "average lunar mare" (~3.4 Gyr for NPF) and the ratio of NPF/HPF for Mars and moon.

D_L (km)	$N_H(Mars)$	$N_H(moon)$	$(NPF/HPF)_{Mars}$	$(NPF/HPF)_{moon}$
0.0156	8154	19210	0.21	0.15
0.0221	2170	5113	0.26	0.20
0.0313	577.4	1360	0.32	0.25
0.0442	153.6	362	0.41	0.31
0.0625	40.88	96.32	0.51	0.39
0.0884	10.88	25.63	0.65	0.49
0.1250	2.895	6.82	0.79	0.62
0.1768	0.7702	1.815	0.91	0.77
0.2500	0.205	0.4829	0.99	0.89
0.3536	0.05454	0.1285	1.02	0.98
0.5000	0.01451	0.03419	1.03	1.02
0.7071	3.787×10^{-3}	9.098×10^{-3}	1.09	1.03
1.0000	1.158×10^{-3}	2.421×10^{-3}	1.04	1.06
1.414	6.207×10^{-4}	6.443×10^{-4}	0.62	1.14
2.000	3.326×10^{-4}	3.453×10^{-4}	0.42	0.67
2.828	1.782×10^{-4}	1.850×10^{-4}	0.33	0.45
4.000	9.552×10^{-5}	9.915×10^{-5}	0.29	0.34
5.657	4.902×10^{-5}	5.313×10^{-5}	0.31	0.30
8.000	2.580×10^{-5}	2.847×10^{-5}	0.39	0.31
11.310	1.646×10^{-5}	1.526×10^{-5}	0.53	0.38
16.000	8.821×10^{-6}	8.177×10^{-6}	0.74	0.54
22.630	4.727×10^{-6}	4.382×10^{-6}	0.90	0.74
32.000	2.533×10^{-6}	2.348×10^{-6}	0.92	0.90
45.250	1.357×10^{-6}	1.258×10^{-6}	0.78	0.91
64.000	6.336×10^{-7}	6.736×10^{-7}	0.66	0.78
90.510	2.956×10^{-7}	3.142×10^{-7}	0.52	0.66
128.000	1.379×10^{-7}	1.466×10^{-7}	0.41	0.52
181.000	6.433×10^{-8}	6.839×10^{-8}	0.33	0.41
256.000	3.001×10^{-8}	3.191×10^{-8}	0.35	0.32

TABLE III

Coefficients for the Martian NPF

n	a_n	n	a_n	n	a_n	n	a_n
0	-3.384	3	0.7915	6	0.1016	9	-4.753×10^{-3}
1	-3.197	4	-0.4861	7	6.756×10^{-2}	10	6.233×10^{-4}
2	1.257	5	-0.3630	8	$-1.181\cdot10^{-2}$	11	5.805×10^{-5}

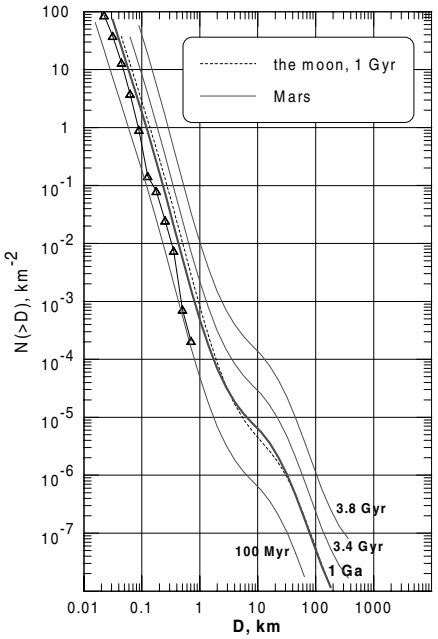

Figure 7. The Martian "isochrones" based on the Neukum Production Function (**Model 1**) with the gravity/collapse (no strength/gravity transition) scaling of cratering. The dashed line presents the 1 Gyr isochron for the moon. The detailed Mars-to-moon comparison is shown in Figure 5. The same data as in Figure 5 for the caldera floor of Arsia Mons are shown for comparison.

The coefficient a_0 in Table III is calculated for a crater retention age of 1 Gyr. It corresponds to the cumulative number of craters larger 1 km

$$N(1) = 10^{-3.312} = 4.13 \times 10^{-4} \text{ km}^{-2} .$$

Using the same time dependence as for the moon (Neukum, 1983; Neukum *et al.*, 2001) one can propose the similar time dependence for Mars

$$N(1) = 2.68 \cdot 10^{-14}(\exp(6.93T) - 1) + 4.13 \times 10^{-4}T \quad . \tag{13}$$

The introduction of a possible strength/gravity transition into the cratering scaling law adds some difference in the Mars-to-moon ratio of crater numbers. Figure 5 shows that in this case the Mars-to-moon ratio should increase to the one for crater diameters near $D = 10$ m.

Conclusions. According to the models described above, the impact crater number on Mars does not differ more than $\pm 50\%$ from the lunar crater number in the same diameter bins. The more frequent asteroid impacts on Mars do not result in a much larger cratering rate: the larger surface gravity and the smaller impact velocity decrease the crater size compared to the impact of the same body on the moon. Finally, the cratering rate Mars-moon ratio varies in the range $0.6 - 1.2$, depending on the steepness of the $N(D)$ distribution.

References

R.P. Binzel, T. Gehrels, and M.S.Matthews (eds).: 1989, *Asteroids II*, Univ. Arizona Press, Tucson.

Bottke, W.F., Jr., Morbidelli, A., Petit, J.M., Gladman, B., and Jedicke, R.: 2000a, 'Tracking NEAs from Their Source Regions to Their Observed Orbits', *Proc. 31st Lunar Planet Sci. Conf.*, abstract #1634.

Bottke, W.F., Jr., Jedicke, R., Morbidelli, A., Petit, J.M., and Gladman, B.,: 2000b, 'Understanding the Distribution of Near-Earth Asteroids', *Science* **288**, 2190–2194.

Bottke, W.F., Love, S.G., Tytell, D., and Glotch, T.: 2000c, 'Interpreting the Elliptical Crater Populations on Mars, Venus, and the Moon', *Icarus* **145**, 108–121.

Chapman, C.R., and McKinnon, W.B.: 1986, 'Cratering of Planetary Satellites', *Satellites*, Univ. Arizona Press, Tucson, pp. 492–580.

Croft, S.K.: 1985, 'The Scaling of Complex Craters', *J. Geophys. Res.* **90**, 828–842.

Farinella, P., Froeschle, Ch., Froeschle, C., Gonczi, R., Hahn, G., Morbidelli, A., and Valesechhi, G.B.: 1994, 'Asteroids Falling Into the Sun', *Nature* **371**, 314–317.

Garvin, J.B., Frawley, J.J., Sakimoto, S.E.H., and Schnetzler, C.: 2000, 'Global Geometric Properties of Martian Impact Craters: An Assessment from Mars Orbiter Laser Altimeter (MOLA) Digital Elevation Models', *Proc. 31st Lunar Planet Sci. Conf.*, abstract #1619.

Gault, D.E., and Wedekind, J.A.: 1978, 'Experimental Studies of Oblique Impact', *Proc. 9th Lunar Planet. Set. Conf.*, Pergamon Press, New York, pp. 3843–3875.

Gladman, B.J., *et al.*: 1997, 'Dynamical Lifetimes of Objects Injected Into Asteroid Main Belt Resonances', *Science* **277**, 197–201.

Greenberg, R., and Nolan, M.: 1989, 'Delivery of Asteroids and Meteorites to the Inner Solar System', *in* R.P. Binzel *et al.* (eds.), *Asteroids II*, Univ. Arizona Press, Tucson, pp. 778–804.

Greenberg, R., and Nolan, M.: 1993, 'Dynamical Relationships of Near-Earth Asteroids to Main-belt Asteroids', *Resources of Near-Earth Space*, Univ. Arizona Press, Tucson, pp. 473–492.

Grieve, R.A.F., and Cintala, M.J.: 1992, 'An Analysis of Differential Impact Melt-crater Scaling and Implications for the Terrestrial Impact Record', *Meteoritics* **27**, 526–538.

Hartmann, W.K.: 1977, 'Relative Crater Production Rates on Planets', *Icarus* **31**, 260–276.

Hartmann, W.K.: 1999, 'Martian Cratering VI. Crater Count Isochrons and Evidence for Recent Volcanism from Mars Global Surveyor', *Met. Planet. Sci.* **34**, 167–177.

Hartmann, W.K., and Neukum, G.: 2001, 'Cratering Chronology and the Evolution of Mars', *Space Sci. Rev.*, this volume.

Hartmann, W.K., *et al.*: 1981, 'Chronology of Planetary Volcanism by Comparative Studies of Planetary Craters', *in* W.M. Kaula, R.B. Merrill, and R. Ridings (eds.), *Basaltic Volcanism at the Terrestrial Planets*, Pergamon Press, New York, pp. 1050–1127.

Ivanov, B.A.: 1981, 'Cratering Mechanics', *Adv. Sci. Techn. VINITI, Mechanics of Deformable Solids* **14**, Moscow, VINITI Press, pp. 60–128, in Russian; English translation: NASA Tech. Memorandum 88477/N87-15662, 1986.

Ivanov, B.A.: 1999, 'Target – Earth. Size Frequency Distribution of Asteroids and Impact Craters', *Proc. Institute for Dynamic of Geospheres*, Moscow, Russia (in Russian), pp. 33–44.

Ivanov, B.A., Neukum, G., and Wagner, R.: 1999, 'Impact Craters, NEA, and Main Belt Asteroids: Size-frequency Distribution', *Proc. 30th Lunar Planet. Sci. Conf.*, abstract #1583 (CD-ROM).

Ivanov, B.A., Neukum, G., and Wagner, R.: 2000, 'Size–Frequency Distributions of Planetary Impact Craters and Asteroids', *in* H. Rickman, and M. Marov (eds.), *Collisional Processes in the Solar System*, ASSL, Kluwer Academic Publishers, Dordrecht, in press.

Jedicke, R., and Metcalfe, T.S.: 1998, 'The Orbital Absolute Magnitude Distributions of Main Belt Asteroids', *Icarus* **131**, 245–260.

Melosh, H.J., and Ivanov, B.A.: 1999, 'Impact Crater Collapse', *Ann. Rev. Earth Planet. Sci.* **27**, 385–415.

Migliorini, F.P., Michel., P., Morbidelli, A., Nesvorny, D., and Zappala, V.: 1998, 'Origin of Earth-crossing Asteroids: The New Scenario', *Science* **281**, 2022–2024.
Morbidelli, A.: 1999, 'Origin and Evolution of Near-Earth Asteroids', *Celestial Mech. and Dynamical Astron.* **73**, 39–50.
Neukum, G.: 1983, *Meteoritenbombardement and Datierung planetarer Oberflächen*, Habilitation dissertation for faculty membership, Univ. of Munich, 1983, 186 pp.
Neukum, G., and Ivanov, B.A.: 1994, 'Crater Size Distributions and Impact Probabilities on Earth from Lunar, Terrestrial Planet, and Asteroid Cratering Data', *in* T. Gehrels (ed.), *Hazards due to Comets and Asterois*, Univ. Arizona Press, Tucson, pp. 359–416.
Neukum, G., Ivanov, B., and Hartmann, W.K.: 2001, 'Cratering Records in the Inner Solar System in Relation to the Lunar Reference System', *Space Sci. Rev.*, this volume.
Pierazzo, E., Vickery, A.M., and Melosh, H.J.: 1997, 'A Re-evaluation of Impact Melt Production', *Icarus* **127**, 498–423.
Pike, R.J.: 1980, 'Control of Crater Morphology by Gravity and Target Type: Mars, Earth, moon', *Proc. 11th Lunar. Planet Sci. Conf.*, Pergamon Press, New York, pp. 2159–2189
Rabinowitz, D.: 1993, 'The Size-distribution of the Earth-approaching Asteroids', *Astrophys. J.* **407**, 412–427.
Rabinowitz, D.L.: 1997, 'Are Main-belt Asteroids a Sufficient Source for the Earth-approaching Asteroids? Part II. Predicted vs. Observed Size Distribution', *Icarus* **130**, 287–295.
Rabinowitz, D., Bowell, E., Shoemaker, E., and Muinonen, K.: 1994, 'The Population of Earth-crossing Asteroids', *in* T. Gehrels (ed.), *Hazards due to Comets and Asteroids*, Univ. Arizona Press, Tucson, pp. 285–312.
Roemer, E.: 1965, 'Observations of Comets and Minor Planets', *Astron. J.* **70**, 397–402.
Roemer, E.: 1966, 'The Dimensions of Cometary Nuclei', *Les Congrès et Colloques de Université de Liège* **37**, Université de Liège, pp. 23–28.
Roemer, E., and Lloyd, R.E.: 1966 'Observations of Comets, Minor Planets and Satellites', *Astron. J.* **71**, 443–457.
Roemer, E., Thomas, M., and Lloyd, R.E.: 1966 'Observations of Comets, Minor Planets, and Jupiter VIII', *Astron. J.* **71**, 591–601.
Schmidt, R.M, and Housen, K.R.,: 1987, 'Some Recent Advances in the Scaling of Impact and Explosion Cratering', *Int. J. Impact Engng.* **5**, 543–560.
Shoemaker, E.M., and Wolfe, R.F.: 1982, 'Cratering Time Scales for the Galilean Satellites', *in* D. Morrison (ed.), *Satellites of Jupiter*, Univ. Arizona Press, Tucson, pp. 277–339.
Ward, W.R.: 1992, 'Long-term Orbital and Spin Dynamics of Mars', *in* H.H. Kieffer, B.M. Jakovsky, C.W. Snyder, and M.S. Matthews (eds.), *Mars*, Univ. Arizona Press, Tucson, pp. 298–320.
Wetherill, G.W.: 1967 'Collisions in the Asteroid Belt', *J. Geophys. Res.* **72**, 2429–2444.
Wetherill, G.W.: 1979 'Steady-state Population of Apollo-Amor Object', *Icarus* **37**, 96–112.
Wetherill, G.W.: 1988, 'Where do the Apollo Objects Come From?', *Icarus]* **76**, 1–18.
Wetherill, G.W.: 1989, 'Origin of the Asteroid Belt', *in* R.P. Binzel *et al.* (eds.), *Asteroids II*, pp. 661–680.

Address for correspondence: Institute for Dynamics of Geospheres, Russian Academy of Sciences, Leninsky Prospect 38/6, Moscow, Russia 117939;
(baivanov@idg.chph.ras.ru)